Ocean-atmosphere variability related with the midsummer drought over Mexico and Central America in the CFSR reanalysis

Ivonne García Martínez & Julio Sheinbaum
Department of Physical Oceanography, CICESE, Mexico
igarcia@cicese.edu.mx

1 ABSTRACT

The spatial and temporal presence of the midsummer drought (MSD) is investigated by means of the Climate Forecast System Reanalysis (CFSR) for the 1979-2010 period. The seasonal migration of the Intertropical Convergence Zone (ITCZ) and the intensification of the Caribbean Low Level Jet (CLLJ) seem to be the key factors involved in the dynamics of the MSD. Furthermore, the results strongly suggest that the MSD might be not only the result of a rain suppressor mechanism (as documented until now) but, in addition, that it might be a manifestation of the reinforcement of the rain at the beginning and at the end of summer season.

2 OBJECTIVE

Establish the atmospheric and oceanic configuration patterns to better understand the mechanism behind the summer precipitation by means of the CFSR coupled reanalysis.

3 DATA

Data from the CFSR for the 1979-2010 period were taken from the NCAR Research Data Archive Website (http://rda.ucar.edu/datasets/ds093.0). The time resolution is 6 hours and the spatial resolutions are 0.5° and 0.3° (depending on availability).

4 MSD SIGNAL

The bimodal signal of the MSD was first detected in space through a biweekly climatology for 5°x 5° regions (Fig. 1). Then, considering only this MSD region, a objective method was developed to select the years with intense MSD (Fig. 2).

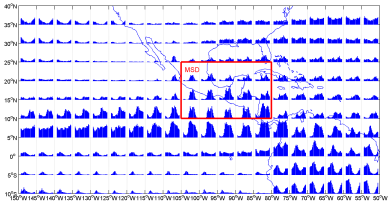

Fig. 1 Climatological distribution of biweekly precipitation rates [mm(2 weeks)$^{-1}$] for 5°x5° regions. The MSD Region is enclosed in a red box.

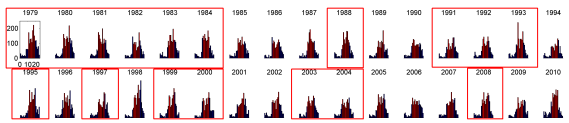

Fig. 2 Annual precipitation distribution rates [mm(2 weeks) $^{-1}$] in the MSD region. Red bars correspond to June-September period.

5 OCEAN-ATMOSPHERE EVOLUTION IN SUMMERTIME

Summer season was classified into three phases, where phase 1 is the first maximum of precipitation, phase 2 the MSD and phase 3 the second maximum. Anomaly fields (Fig. 3) were obtain subtracting June, July-August and September climatologies from phases 1, 2 and 3, respectively.

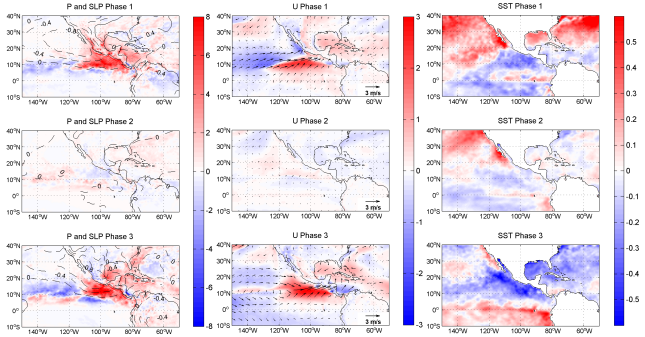

Fig. 3 Anomalies of MSD years for precipitation [*P*] (mm day^{-1}, color), sea level pressure [*SLP*] (mb, contours), 10-m wind [*U*] (ms^{-1}) and sea surface temperature [*SST*] (°C).

This procedure allows one to compare the behavior of physical variables in the MSD years with their climatological values. The more intense anomalies were found in wet phases (1 and 3), while the composite of phase 2 has the same behavior as the July-August climatology, suggesting that the bimodal distribution of precipitation is mainly due to the intensity of the two maxima, more than the diminution during the MSD itself.

To quantify oceanic changes during MSD years, the warm pool (WHWP) extension was measured. A reduction during MSD years (more pronounced in midsummer) was found, while an increase in the years when MSD is weak or non existent occurs (Fig. 4).

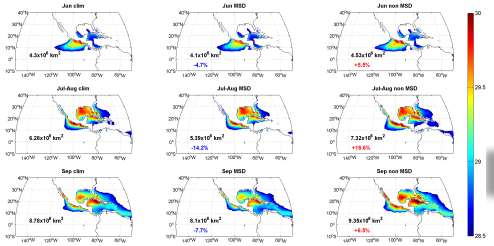

Fig. 4 *SST* (°C) and extension (km^2) of the WHWP in: 1979-2010 climatology, composite of MSD years and composite of years with no MSD for June, July-August and September. At the bottom left corner of each map the area covered by the WHWP and its change percentaje (respect to the climatology) are indicated.

6 CAUSE-EFFECT RELATIONSHIPS

In order to find cause-effect relationships with greater accuracy, a quantitative method proposed by Liang (2014) was applied. This method evaluates the information flow between two time series, X_1 and X_2. The rate of information flowing from X_2 to X_1 is given by:

$$T_{2\to1} = \frac{C_{11}C_{12}C_{2,d1} - C_{12}^2 C_{1,d1}}{C_{11}^2 C_{22} - C_{11}C_{12}^2}$$

Where C_{ij} is the sample covariance between X_i and X_j, and $C_{i,dj}$ is the sample covariance between X_i and $(X_{j,n+1}-X_j)/dt$, where dt is the timestep. If $|T_{2\to1}|$ is nonzero, X_2 is causal to X_1; otherwise is non causal.

Information flow was computed for precipitation in the MSD region (*P*) and two variables: 1) *SST* and 2) 10-m zonal wind (*u*) (Fig. 5). July-August *SST* in the Caribbean Sea makes *P* more uncertain in the MSD region (a). In contrast, the low information flow from *P* to Caribbean *SST* (b) indicates no causal relationship. For the same period, *u* and *P* are mutually causal: *u* is a source of uncertainty for *P* (c), while precipitation in the MSD region tends to stabilize *u* (d).

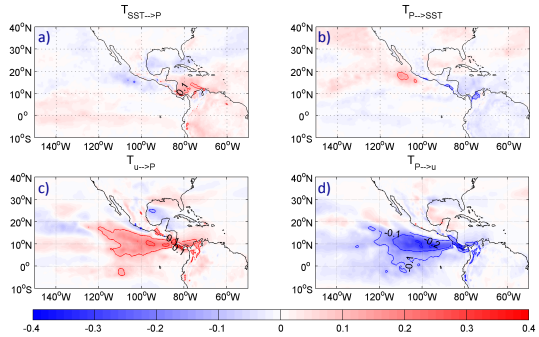

Fig. 5 Information flow [nats (2 weeks) $^{-1}$] between (up) SST and P and (down) *u* and *P* in the MSD region for July-August.

Some of the information flow patterns can be translated into direct physical mechanisms, however, others are more complex and need further research.

7 REFERENCES

San Liang, X. (2014). Unraveling the cause-effect relation between time series. *Physical Review E*, *90*(5), 052150.